2015

Mast Cells In Kainate Receptor Knockout Mice

Andrea J. Elkovich
Virginia Commonwealth University

MAST CELLS IN KAINATE RECEPTOR KNOCKOUT MICE

A thesis submitted in partial fulfillment of the requirements for the degree of
Master of Science at Virginia Commonwealth University

by

ANDREA J. ELKOVICH
Bachelors of Science– Virginia Commonwealth of University, 2011

Director: Daniel Conrad, Ph.D. Professor
VCU Department of Microbiology & Immunology

Virginia Commonwealth University
Richmond, VA
June 2015

-Acknowledgements-

They tell us during our rotations to find a lab where we "fit in" and this is probably the best advice we get. Thank you Dr. Conrad for accepting me into your lab, despite having never picked up a pipette, let alone a mouse. Dr. Jamie Sturgill, thank you for working with me from the beginning and allowing me to further delve into the KAR KO story. Dr. Rebecca Martin, thank you for taking me under your wing during my rotation and beyond. Looking back at how you interact and teach new lab members, I know your positive attitude has shaped me and many others into fine young scientists. Sheela Damle, PhDc; thank you for not laughing too hard at my mistakes, and always giving me sound advice when I need it. To the rest of the Conrad Lab members, past and present: Dr. Lauren Cooley, Hannah Zellner, Becky Keim (aneth ara), and Joe Lownik. Thank you for all the laughs and making lab a fun place to be every day.

To Dr. Ryan, thank you for allowing me to rotate last spring and for helping me along the way with the mast cells that are so foreign to our B cell lab. Dr. Jamie McLeod, you've been such a big help and I look forward to continuing our collaboration. Brian Barnstein and Dana Curley, thank you for your guidance and patience!

To my parents, Liz and Paul Elkovich, thank you for the constant support, especially financially; bagels and coffee are just as big an investment as tuition. To Laura, Rudy, and Rylan Samaroo, thank you for the laughs and utter chaos. To the animals in my life: Oscar, Peaches, and Zazu—your pictures decorate my office wall and give me smiles throughout the day.

-Table of Contents-

-List of Figures-

Page

-List of Abbreviations-

α	alpha
γ	gamma
δ	delta
ε	epsilon
κ	kappa
λ	lambda
μ	mu
μM	micro-molar
μm	micron
AADES	Aortic Adventitia Digestion Enzyme Solution
ADES	Aorta Dissociation Enzyme Solution
Ag	Antigen
AHR	Airway Hyperreactivity
APC (immune cell)	Antigen-Presenting Cell
APC (fluorophore)	Allophycocyanin
Beta-hex	Beta-Hexosaminidase
BMMC	Bone Marrow-derived Mast Cell
BSA	Bovine Serum Albumin
Ca^{2+}	Calcium ion
CD	Cluster of Differentiation
CFA	Complete Freund's Adjuvant
CNS	Central Nervous System
CRAC	Calcium Release Activated Channels
DAG	Diacylglycerol
DAR	Department of Animal Research
DNP	Dinitrophenol
ELISA	Enzyme-Linked ImmunoSorbant Assay
Fab	Fragment, antigen-binding
FACS	Fluorescence-Activated Cell Sorting
FBS	Fetal Bovine Serum
Fc	Fragment, crystallizable
FcR	Fragment, crystallizable Receptor
FITC	Fluorescein isothiocyanate
G	Tissue dampening
Glu	Glutamate
GluR	Glutamate Receptor
H	Elastance
HDM	House Dust Mite
HR	Histamine Receptor
IACUC	Institutional Animal Care and Use Committee
IFA	Incomplete Freund's Adjuvant
IFN	Interferon

Ig	Immunoglobulin
IL	Interleukin
I.P.	Intraperitoneal
IP_3	Inositol trisphosphate
ITAM	Immuno-receptor Tyrosine-based Activation Motif
KA	Kainic Acid
KAR	Kainate Receptor
kDa	kilo-Dalton
KO	Knockout
LAMP-1	Lysosomal-Associated Membrane Protein-1
LAT	Linker for Activation of T cells
LPS	Lipopolysaccharide
MAPKKK	Mitogen-Activated Protein Kinase Kinase Kinase
MAPKK	Mitogen-Activated Protein Kinase Kinase
MAPK	Mitogen-Activated Protein Kinsase
mg	mili-gram
mL	mili-liter
mM	mili-molar
Nb	*Nippostrongylus brasiliensis*
ng	nano-grams
NP-KLH	4-hydroxy-3-nitrophenyl acetyl-keyhole lympet hemocyanin
PAMP	Pathogen-Associated Molecular Patterns
PBS	Phosphate Buffered Saline
PCA	Passive Cutaneous Anaphylaxis
PE (histology)	Pinacyanol Erythrocyanate
PE (fluorophore)	Phycoerythrin
PIP_2	Phosphatidylinositol (4, 5)-bisphosphate
PKC	Protein Kinase C
PLA2	Phospholipase A2
PLC	Phospholipase C
PNAG	p-Nitrophenyl N-acetyl-β-D-glucosaminide
PSA	Passive Systemic Anaphylaxis
R_n	Newtonian Resistance
RPM	Revolutions Per Minute
RSV	Rous Sarcoma Virus
SCF	Stem Cell Factor
SD	Standard Deviation
SOC	Store Operated Calcium
Src	Sarcoma
STIM	Stromal Interaction Molecule
TCFG-2	T Cell Growth Factor 2
T_H	T helper
TNF	Tumor Necrosis Factor
TLR	Toll-Like Receptor
W/O	Water-In-Oil
WT	Wild Type

Abstract

MAST CELLS IN KAINATE RECEPTOR KNOCKOUT MICE

Andrea J. Elkovich
Bachelors of Science– Virginia Commonwealth of University, 2011

A thesis submitted in partial fulfillment of the requirements for the degree of Master of Science at Virginia Commonwealth University

Virginia Commonwealth University, 2015

Director: Daniel Conrad, Ph.D. Professor
VCU Department of Microbiology & Immunology

Kainate receptor knockout mice have unique differences within their immune system. They exhibit an attenuated T_H2 branch, while maintaining a robust T_H1 response. Specifically, blocking the formation of functional kainate receptors affects mast cells and their related pathologies. While they seem to develop and activate normally *in vivo* and *in vitro*, KAR KO mast cells release more inflammatory mediators upon degranulation. These mice experience severe anaphylactic shock due to two compounding abnormalities. First, KAR KO mast cells release significantly more histamine *in vivo* upon IgE-mediated activation. Second, the animals over-respond to exogenous histamine with drastic temperature drops compared to WT.

-Chapter 1: Introduction-

Allergies and the Immune System

Atopic disease, or Type I Hypersensitivity, is an IgE-mediated immune response against innocuous environmental antigens[1]. Due to a combination of genetic and environmental factors, certain individuals are prone to producing excessive IgE antibodies against common allergens such as pollen or dander[1,2]. These antibodies then become localized in the tissue by binding their high affinity receptor, FcεRI, on resident mast cells. Upon re-exposure to multivalent antigen, the IgE becomes cross-linked and activates the mast cells to release pro-inflammatory mediators, leading to the well-known symptoms of IgE-mediated allergic disease

Mast cell activation is biphasic and therefore gives rise to different clinical symptoms classified as either from the early or late response[2–4]. Seconds after IgE is cross-linked, the activating signal causes the mast cell to degranulate. This immediate release of pre-formed mediators causes the characteristic symptoms of allergic reaction shown below in Figure 1-1.

	Mediators Released	Physiological Effect	Symptoms
Early Phase	Vasoactive amines (histamine, seratonin), proteoglycans (heparin,), proteases (tryptase, chymase)	Increased vascular permeability, smooth muscle contraction, mucus production/secretion	Airway obstruction/wheezing, congestion, edema, temperature/blood pressure drop
Late Phase	*De novo* synthesis of eicosanoids, chemotractants, cytokines	Immune cell recruitment/ activation, second round of smooth muscle contraction, vasodilation / permeability	Chronic inflammation, tissue remodeling, airway hyperreactivity

Figure 1-1. Mast cell mediators cause allergic symptoms.

Following activation, *de novo* synthesis slowly produces and releases molecules that will facilitate the late phase. Originally derived from membrane phospholipids, arachidonic acid is converted into prostaglandins, thromboxanes, and leukotrienes. This group of lipid mediators is collectively known as eicosanoids (Figure 1-2).

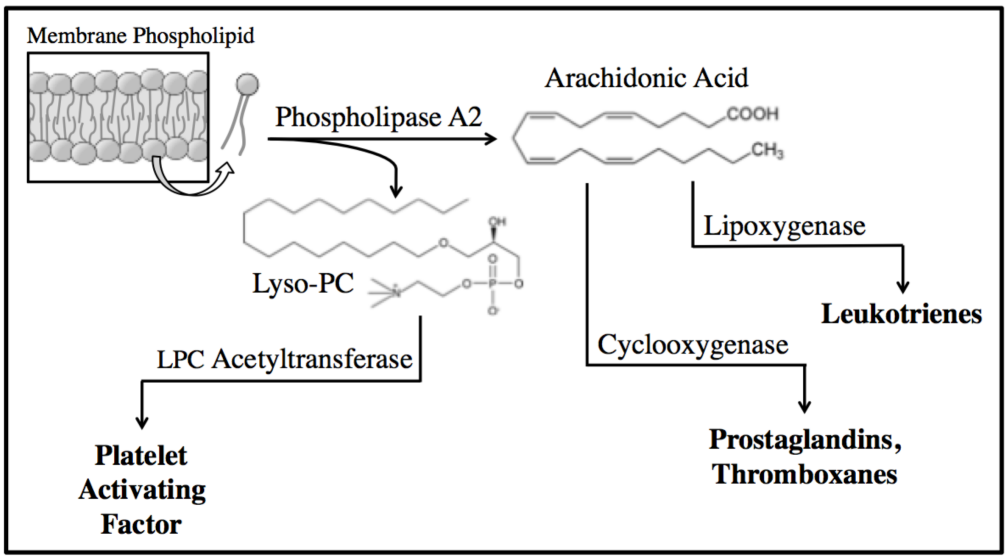

Figure 1-2. *De novo* synthesis of eicosanoids.
PLA2 converts membrane phospholipids into arachidonic acid and lyso-PC. Arachidonic acid is metabolized into leukotrienes, prostaglandins, and thromboxanes. Lyso-PC is the precursor for platelet activating factor.

In combination with other delayed-release cytokines, the late phase is marked by the influx and activation of leukocytes four to six hours later. Eosinophilia and the general inflammatory environment facilitates a second round of smooth muscle contraction and prolonged edema. In anaphylaxis, this presents with abdominal pain and shortness of breath[5]. In the asthma, this can contributes to airway remodeling and the development of airway hyperreactivity (AHR), especially if the antigen persists. Eventually this state of chronic inflammation leaves the body susceptible to flare-ups triggered by unrelated environmental irritants such as smoke[4].

Although a large portion of society in developed countries suffers from allergies today, this T_H2 type of immunity originally evolved from humanity's battle against multicellular parasites. Mast cells stand guard at vulnerable entry points of invasion, specifically clustered around vessels in mucosal and epithelial tissues[6]. A common defense against intestinal infections, such as *Heligmosomoides polygyrus*, is the STAT6-mediated "weep and sweep." This process involves increased luminal secretions—weep, and contractility—sweep, intended to expel the worms[6]. Recruited immune cells can accumulate to form granulomas around the physical invaders or release mediators to directly damage them[6]. Such protective effects, however, become harmful during inappropriate activation by allergens. The acute inflammation triggered by mast cells and eosinophils is meant to resolve upon parasite clearance. Ubiquitous environmental allergens, however, cause persistent inflammation with harmful effects; in essence, the body's protective response becomes destructive, causing irreversible tissue damage in chronic diseases[2].

Systemic anaphylaxis is the most severe example of an inappropriate immune response. The reaction progresses rapidly, causing extensive vascular fluid loss that results in respiratory or cardiovascular collapse and even death[7]. Mast cell degranulation is again responsible for the sudden onset as well as the delayed wave of symptoms. Because this condition is systemic, the vasoactive mediators cause a devastating drop in blood pressure and temperature that can be used to gauge the severity of the reaction.

Balance Between T_H1 and T_H2

The paradigm between T_H1 and T_H2 immunity stems from a 1986 publication that described the cytokine patterns of two divergent helper T cell populations[8]. Mosmann et al.

characterized Type I T cells by IL-2 and IFN-γ production and Type II T cells by IL-4 (reported as MCGF-2) and T Cell Growth Factor 2 (TCFG-2). The Type II clone was further characterized by its ability to elicit polyclonal IgE and IgG1 production by lipopolysaccharide (LPS)-stimulated B cells[8]. This group also coined the terms T_H1 and T_H2 that we use today.

IFN-γ and IL-2 are now recognized as classic T_H1 cytokines that direct immune responses against viruses and other intracellular pathogens. T_H2-derived IL-4 and IL-5 command the humoral response against multicellular parasites and extracellular pathogens. It is important to mention that we also recognize a plethora of other T cell subtypes (T_H0, T_H17, T_{regs}); what binds T_H1/T_H2 together is their ability to up-regulate their own activities, while repressing their counterpart[9]. Figure 1-3 demonstrates how T_H2 cells secrete IL-10, which blocks the production of IFN-γ, and IL-4 further skews toward a T_H2 environment. T_H1-produced IFN-γ, on the other hand, blocks T_H2 cells from proliferating, while secreting self-enhancing IL-2.

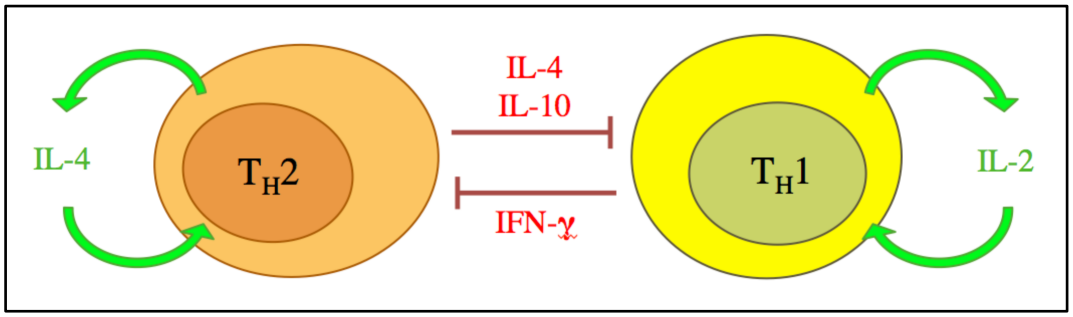

Figure 1-3. Balance between T_H1 and T_H2 skewing of the immune system. Both cell types produce cytokines to enhance themselves while also blocking the other.

This balance of power is often used as a simplified dogma or foundation to study the complex interactions between immune components[9]. According to the paradigm, we assume there is a resting homeostasis between the two branches. Upon antigen challenge, naïve T_H0 cells become polarized toward the branch which is appropriate for clearance. When all goes

well and the cell is committed, the irrelevant branch is weakened so that the appropriate branch can mount a robust response.

T_H2 Infection Model

Hailing from the phylum Nematoda, *Nippostrongylus brasiliensis* (*Nb*) is a parasite of rodents. Similar to the human hookworm, *Nb* establishes infection within the host's intestines for the purpose of reproducing; its life cycle shown in Figure 1-4. Secreted cytokines, including IL-4, 5, 9, and 13, direct the protective response toward IgE production, eosinophilia, mucosal mast cell expansion, and mucus production[6]. Together, this previously mentioned "weep-and-sweep" defense succeeds in expelling the worms within two weeks. Although localized within the mucosa, the infection triggers a systemic T_H2 immune response, making it an ideal model to study *in vivo*[13].

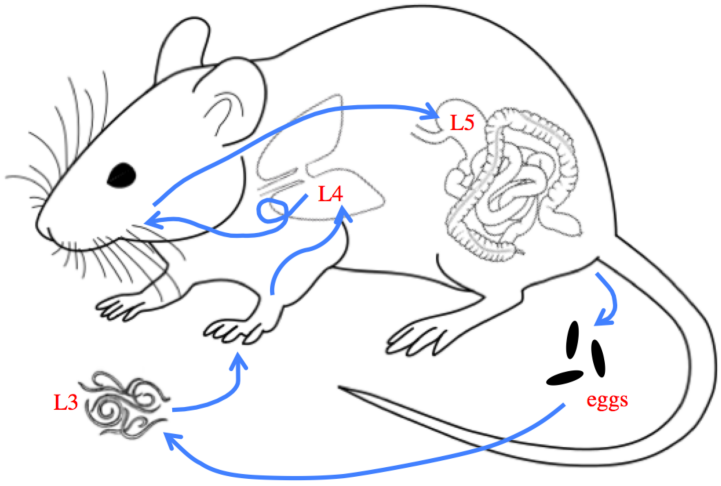

Figure 1-4. *Nippostrongylus brasiliensis* life cycle[1].
Stage-3 larvae enter their rodent host through the skin of the footpad. Following the bloodstream, the worms reach the lungs where they mature to stage-4 larvae. The worms are coughed up and subsequently swallowed. Within the small intestines the worms mature to stage-5 and reproduce. Eggs become incorporated into the feces.

[1] Image a combination and adaptation of external sources[10–12]

T_H1 Model

Lydia Rabinowitsch was the first to report the formation of tubercles at the injection site of fatty substances. She found that *Mycobacterium butyricum*, only when incorporated into butter, caused a local granuloma reaction[14]. Intrigued by these results, Jules Freund began to experiment on the use of lanolin-like substances and paraffin oil as adjuvants.

In 1944, Freund published a comprehensive study verifying the benefit of adjuvants in enhancing and sustaining antibody and anti-toxin production. He described the microscopic phenomenon of water-in-oil emulsion, his original drawing shown in Figure 1-5, and noted that the incorporation of heat killed bacteria created an additional synergistic effect[15]. Soon to follow were reports that paraffin oil boosted immediate and long-term virus immunity in experimental animals[16,17] and human influenza vaccines[18].

Freund's research resulted in the emulsion adjuvant that is commonly used today in animals. Freund's Incomplete Adjuvant (IFA) is a water-in-oil (W/O) emulsion of heavy paraffin/mineral oil with an antigen-containing water phase[19]. Because these two substances are immiscible, a surfactant must be added in order to stabilize the interface.

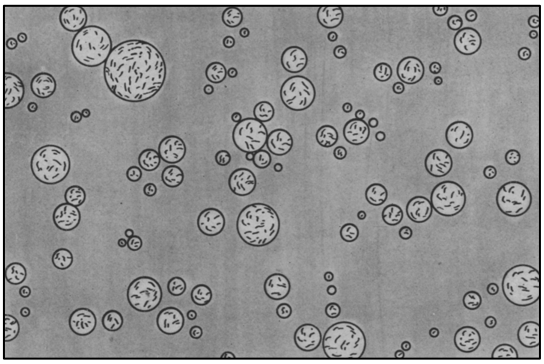

Figure 1-5. Water-in-oil emulsion. As drawn by Jules Freund in his 1944 publication[15].

Mannide monooleates, such as Aralacel A, are lipophilic emulsifying agents that allow tiny aqueous droplets to exist within an oil phase. This final mixture allows for a slow and even release of the suspended antigen, resulting in a prolonged immune response.

Specifically, IFA stimulates the innate immunity to eventually skew toward T_H1, giving rise to the increased resistance to bacterial infection reported by Castro in 1993[20].

Adding heat-killed *Mycobacterium tuberculosis* gives Freund's Complete Adjuvant (CFA). CFA is a much more potent adjuvant because the Pathogen-Associated Molecular Patterns (PAMP) on the bacteria additive activates Toll-Like Receptors (TLR) on antigen-presenting cells (APC). The resulting danger signals lead to a robust T_H1 response[21].

Mast Cell Receptor FcεRI

FcεRI is member of the family of Fc receptors (FcR), which in turn are members of the immunoglobulin supergene family[22,23]. The name and designated Greek letter refer to the fact that these receptors bind the fragment, crystallizable (Fc) portion of different antibody isotypes[1]; for example, FcεRI binds the Fc region of IgE molecules. FcR's are expressed mainly in the myeloid lineage including mast cells, macrophages, and neutrophils, but also on lymphoid B cells and occasionally on non-immune cells like endothelial cells[22,23].

Structurally, FcεRI is a multi-chain complex with the ability to bind ligand and transduce signals. The alpha-chain, shown in blue in Figure 1-6 is a 45kDa protein that directly interacts with circulating IgE[1]. The 33kDa tetra-spanning beta-chain, shown in red, serves a widely accepted role of signal amplification[24,25]. The final component of FcεRI is the 9kDa homodimer gamma chain pair shown in green. The gamma chains are crucial for initiating signal transduction through its ITAMs (Immunoreceptor Tyrosine-based Activation Motifs). Known as a common gamma chain, it is found in other Fc receptors, including FcαRI, FcγRI, III, and IV[1].

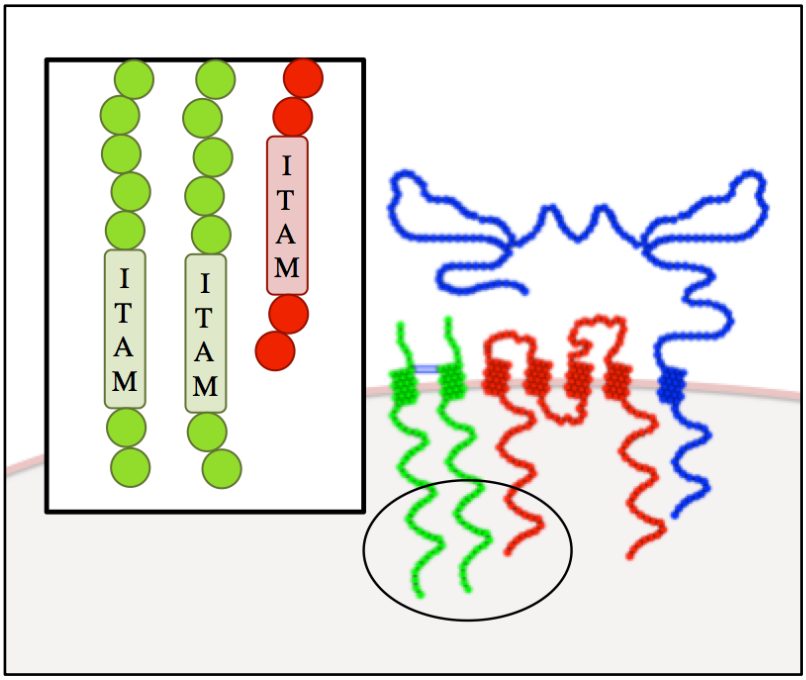

Figure 1-6. Structure of murine FcεRI[2].
Alpha-chain (blue) binds IgE, beta-chain (red) amplifies the signal, gamma-chains (green) initiates signaling. Beta- and gamma-chains contain ITAMs to propagate signaling cascade.

Signaling Through FcεRI

In 1911, pathologist Peyton Rous was experimenting with cancer transmission. In addition to transplanting the malignant mass, he was surprised to find he could also establish tumor in a new host by injecting the cell-free extract from a donor tumor[26]. He hypothesized that a "minute parasitic organism" was responsible for this transmission. This so-called Rous Sarcoma Virus (RSV) became widely studied and eventually lead to the discovery of a single gene that caused cellular transformation[27]. C-Src, named as an abbreviation of sarcoma, is a proto-oncogene that encodes a family of vital signaling enzymes called Src family kinases. Phosphorylation by Src regulates signaling activity by allowing communication between surface receptors with intracellular machinery. Taking a broad look, Src kinases regulate many basic cellular processes such as growth and differentiation[27].

[2] FcεRI adapted from external source

In the case of mast cells, several Src kinases play key roles in proximal activation signaling. Loosely associated with FcεRI, Lyn becomes activated upon receptor aggregation and phosphorylates the tyrosine residues on the beta- and gamma-chain ITAMs[24] shown in Figure 1-6. This creates a high affinity-docking site for Syk, another early activated tyrosine kinase, that will phosphorylate the adaptor molecule LAT (Figure 1-7 A)[24,28]. Linker for Activation of T cells (LAT) serves as a scaffold for the formation of the macromolecular complex required for downstream signaling.

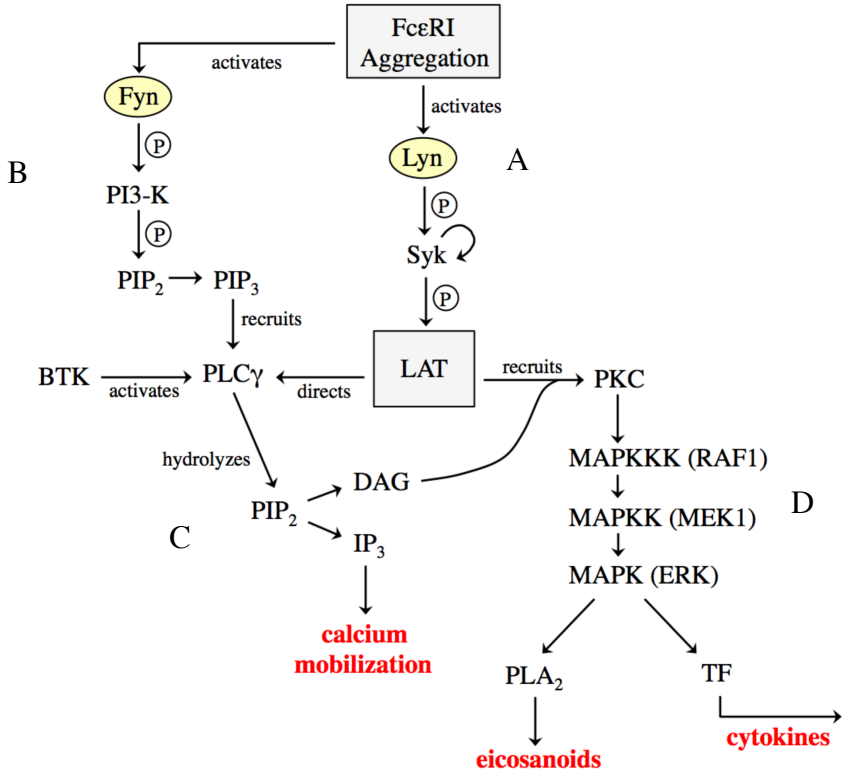

Figure 1-7. Mast cell activation through FcεRI.
A) Receptor aggregation activates Lyn to phosphorylate Syk, which in turn activates LAT.

B) Receptor aggregation also activates Fyn to phosphorylate PI3-K, which in turn phosphorylates PIP_2 to PIP_3. Membrane PIP_3 recruits PLCγ.

C) Upon activation by BTK, LAT directs PLCγ activity to hydrolyze PIP_2 into DAG and IP_3. This splits the signaling down two separate paths. IP_3 triggers calcium mobilization.

D) DAG recruits PKC to LAT, which activates a MAPKKK cascade resulting in cytokine and arachidonic acid production.

Also activated during aggregation is Fyn, the other Src kinase involved in mast cell signaling. Fyn drives a complementary cascade that is separate from the one initiated by Lyn, but both are required for degranulation[29]. Fyn activates Phosphoinositide 3-kinase (PI3-K) indirectly through the membrane protein Gab2[24]. PI3-K adds an additional phosphate group to PIP_2, producing PIP_3.

The main signaling enzyme Phospholipase C-gamma (PLC-γ) is recruited to membrane PIP_3 and activated by BTK. LAT directs PLC-γ activity by its four vital tyrosine residues (Y132, 171, 191, 226). PLC-γ hydrolyzes Phosphatidylinositol (4, 5)-bisphosphate (PIP_2) into Inositol trisphosphate (IP_3) and Diacylglycerol (DAG) (Figure 1-7 C). These two molecules will continue down separate paths leading to calcium mobilization, and PKC activation and degranulation, respectively[25,28].

Membrane-bound DAG helps to localize and activate protein kinase C (PKC) to the plasma membrane. Although not well understood, PKC somehow activates and regulates the multi-tiered MAPK/ERK pathway (Figure 1-7 D). Mitogen-activated protein kinase (MAPK) cascades are an important link between signaling molecules and the nucleus[1]. The final enzyme of the series is able to phosphorylate and activate transcription factors, leading to new gene expression; in the case of mast cells, these genes encode a variety of pro-inflammatory mediators[28]. Additionally, Phospholipase A2 (PLA2) is activated by this relay, allowing eicosanoid production (Figure 1-7 D).

IP_3 induces a transient release of intracellular calcium stores from the endoplasmic reticulum (ER)[28,30] (Figure 1-8). Eventually this limited internal supply runs low, alerting Stromal Interaction Molecule-2 (STIM-2) to communicates with its counterpart STIM-1 on the plasma membrane[31]put. Together, these proteins initiate extracellular calcium influx

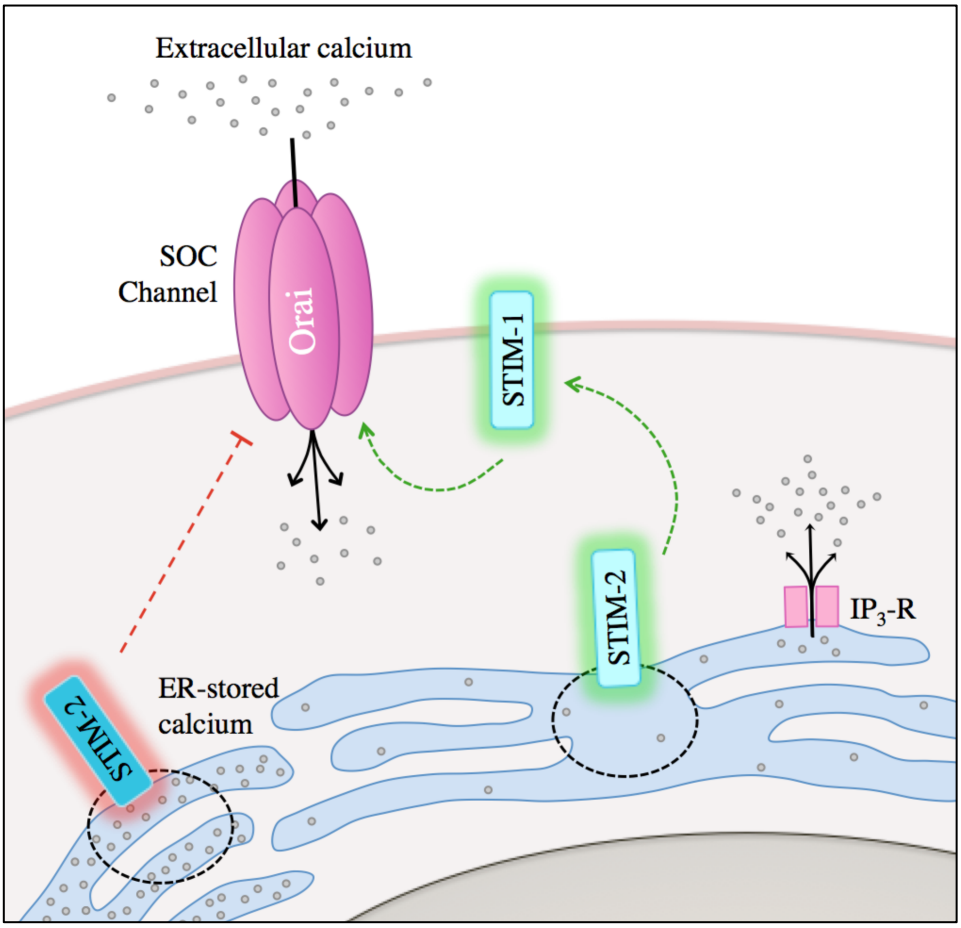

Figure 1-8. Capacitative calcium flux.
IP_3 activates its receptor on the endoplasmic reticulum, opening a channel to release calcium from the lumen. Once the intracellular stores are drained, STIM-2 senses the low [Ca^{2+}] and signals STIM-1 to activate SOC. Also known as CRAC, this channel allows calcium influx to replenish intracellular stores. If ER-stored calcium is at a high enough concentration, STIM-2 remains inactive and SOC is closed to prevent ion flow.

through plasma membrane Store Operated Calcium (SOC) channels[30]. Also referred to as Calcium Release Activated Channels (CRAC), these calcium-selective channels are composed of four pore- forming subunits of the protein Orai[31]. Capacitative calcium entry replenishes the supply, sustaining the calcium flux[28,31]. Calcium signaling within the mast cell will contribute to new gene expression by activating transcription factors[1] and secretion of mediators through granule trafficking[24].

Antibodies

Upon infection or immunization, activated T_H cells can partake in cognate interactions with naïve B cells. Three signals are required to stimulate further B cell activity: 1. CD40-ligand, 2. MHC-II / TCR, 3. secreted cytokines to direct differentiation. Activated B cells can then become plasma cells, which secrete special effector proteins that bind to foreign particles. Known as antibodies, these proteins generally function within the adaptive immune system to neutralize toxins and tag pathogens for destruction by phagocytic cells[1].

The common protein structure, shown in Figure 1-9a, consists of two identical heavy chains (orange) and two identical light chains (yellow). The heavy chains, weighing between 50-73kDa, exist in five classes: A/alpha (α), G/gamma (γ), D/delta (δ), E/epsilon (ε), and M/mu (μ). These isotypes vary depending on four characteristics: number and location of disulfide bonds, number and location of oligosaccharides, number of constant domains, and the length of the hinge region. The light chains, on the other hand, only exist in two forms: lambda (λ) and kappa (κ). Although there is no known functional difference between the two, an antibody will only contain two lambda or two kappa light chains; an antibody never contains one of each[1].

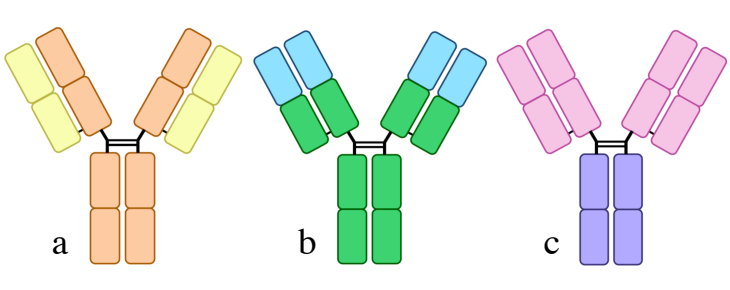

Figure 1-9. Antibody structure.
a. Heavy chain (orange), light chain (yellow)
b. Variable region (blue), constant region (green)
c. F_{ab} (pink), F_c (purple)

The functional region is confined to the c-terminus, known as the constant region, shown in green in Figure 1-9b. Based on the heavy chain's isotype, the constant region determines with which cells the antibody can interact and what immune mechanisms it can initiate. The n-terminal variable region, shown in blue, binds to a distinct antigen epitope that was determined by the unique amino acid sequence of the B cell's receptor (BCR). All antibodies produced by this cell or its daughters will be specific for the same epitope. And although each produces only a single clone, every B cell in the body recognizes a different epitope, allowing the immune system to recognize a huge array of foreign antigens[1].

Another useful way to discuss antibody structure is via the fragments produced by proteolytic cleavage. Papain cleaves around the hinge disulfide bonds, liberating three fragments: two F_{ab} and one F_c. Shown in pink in Figure 1-9c, the two Fragments, antigen-binding (Fab) contain the variable regions. Fragment, crystallizable, shown in purple, contains the constant region that will bind the appropriate F_c receptors for the isotype[1].

As mentioned before, there are five different Ig isotypes, all which originate from a single modular gene, shown schematically in Figure 1-10a. During isotype switching, double-stranded breaks within the DNA allow deletions to be made. Upstream of each constant region, there is a switch region that is acted upon by Activation-Induced Cytidine Deaminase (AID). AID can only access these nucleotides, however, if the DNA strands are separated[1].

In the case of IgE, CD40-L and IL-4 activate STAT6 and NF-κB within the B cell. These transcription factors initiate transcription of their target constant region, epsilon, in order to open the DNA and separate the two strands. At this point, AID is able to come in and convert cytosine residues into uracil via deamination (Figure 1-10a). Uracil DNA

Glycosylase (UNG) and Apyrimidinic Endonuclease-1 (APE-1), proteins involved in DNA repair, will nick the single-stranded DNA at each of these uracils, triggering double-strand break repair machinery. In the end, the two switch regions targeted by AID are joined (Figure 1-10b), while the intervening DNA is cut out (Figure 1-10c). When transcription is initiated at the V region promoter, the epsilon constant region results and IgE is produced[1].

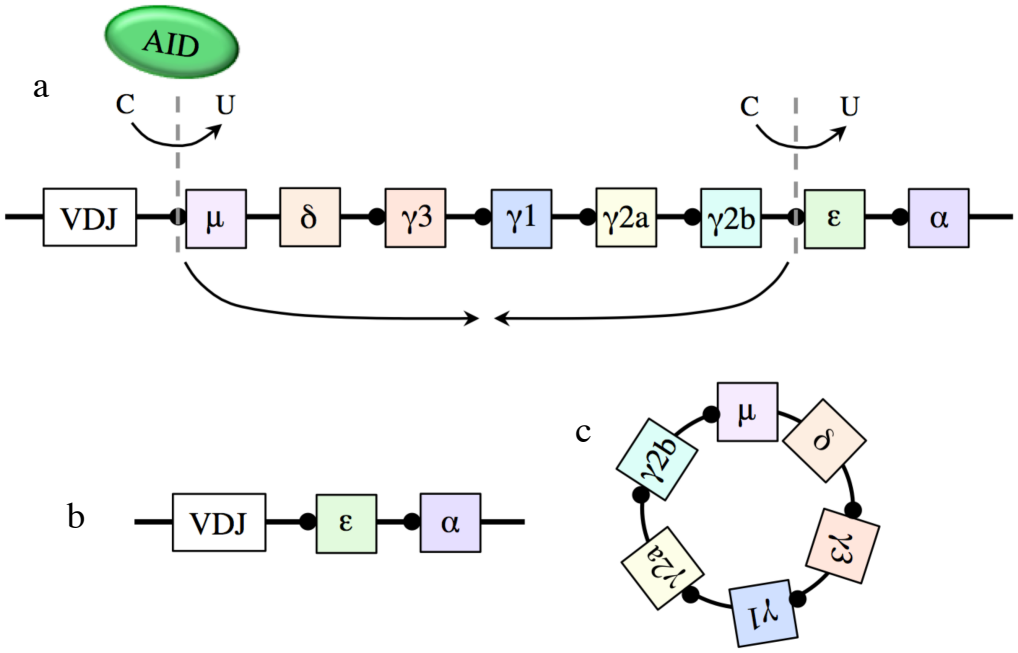

Figure 1-10 IgE isotype switching
AID deaminates random cytosine residues within the switch region to prompt single-strand breaks (a). Upon circularization and excision (c), the epsilon constant region joins with the upstream VDJ component for transcription (b).

Figure 1-11 shows the general structure of IgE. It is a heavily glycosylated, 200kDa protein[32]. Each heavy chain is made up of four subunits or constant domains, one of which takes the place of the hinge region[1]. Of all the isotypes, IgE is the most heavily regulated; in normal circulation, only 10-400 ng/mL will be detected. IgE has a short half-life and

typically decays between 12 hours and two days; binding to an Fc receptor will stabilize the antibody and extend its existence for several weeks[32].

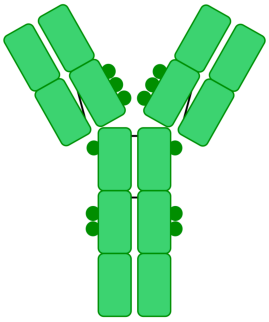

Figure 1-11 IgE protein structure
A 200kDa, heavily glycosylated protein, containing four constant domains with no hinge region.

Glutamate and Its Receptors

Upon discovery of glutamate as the primary excitatory neurotransmitter, research into its receptors (GluR's) began. Glutamate is recognized by a variety of receptors that are firstly divided into an ionotropic or metabotropic class based on their overall structure and function. In general, ionotropic receptors (iGluR) are ligand-gated ion channels that can both bind the neurotransmitter and allow ion flux through its integral channel. Metabotropic receptors (mGluR) do not have a built-in ion channel, so they must signal through a coupled G-protein in order to trigger eventual ion movement[33].

Excitotoxicity in the peripheral tissues was investigated in the mid 1990's by Said, et al. who showed that GluR over-activation could cause lung and airway damage in rats[34]. In this case, the group observed high-permeability pulmonary edema directly related to dose-dependent NMDA treatments. Since then, the group has shown evidence that supports a relationship between iGluR activation and airway inflammation and hyper-reactivity[35].

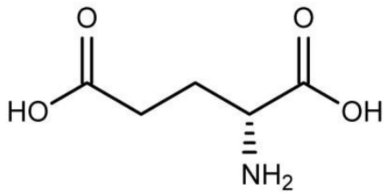

Figure 1-12 Structure of glutamate

Here we focus on ionotropic glutamate receptors (iGluR), which can be further sub-divided into N-methyl-D-Aspartate (NMDA), α-amino-3-hydroxy-5-methyl-4-isoxazolepropionic acid (AMPA), and Kainate (KA). These subtypes are modular and characterized by the heteromeric subunits that make it up, as well as their preferred ligand.

Within the brain, iGluR's participate in fast excitatory synaptic transmission[33]. Studies since the early 1990's, however, have found the existence of peripheral GluR. Circulating glutamate levels can vary between 30-100uM[33], so their presence outside the CNS is not so arbitrary. Many groups have studied the expression and function of peripheral iGluRs on pancreatic islet cells[36], T cells[37], stomach[38], taste receptor cells[39], and many more cell and tissue types. While the NMDA receptor is the focus of much of today's iGluR research, our group studies the often-ignored Kainate receptor (KAR).

This report investigates the phenotype of KAR KO mice, specifically any deficits in atopic disease within the immune system.

-Chapter 2: Materials and Methods-

Section 1: Animals

-Mice

B6/129 colonies were maintained within a VCU Department of Animal Research (DAR) vivarium. Animals of at least six weeks of age were used according to protocols approved by the VCU Institutional Animal Care and Use Committee (IACUC).

-Mouse Euthanasia

All mice were sacrificed by an overdose inhalation of Isoflurane followed by cardiac puncture or cervical dislocation.

Section 2: Bone Marrow Derived Mast Cells

-Mast Cell Media

All mast cells were cultured in complete RPMI 1640 media (Invitrogen Life Technologies – Carlsbad, CA) containing 10% heat-inactivated FBS, 2mM L-Glutamine (cat# SH30034 HyClone- Logan, UT), 1mM Sodium Pyruvate (cat# SH30239 HyClone- Logan, UT), 1mM HEPES (cat# SH30237 HyClone- Logan, UT), 100 units/mL Penicillin G, 100μg/mL Streptomycin (Cat# SV30079 HyClone- Logan, UT), and supplemented with 5ng/mL recombinant IL-3 and 10ng/mL SCF.

-BMMC Culture

Femurs and tibias were surgically removed from deceased mice. The ends of the bones were sliced off to form an open tube. Bone marrow was isolated by centrifugation for five

minutes at 1500 RPM. Red blood cells were removed from the pellet by adding 15mL ACK Lysis Buffer. Cells were washed in 1X PBS then resuspended and maintained at 500,000 cells/mL in Mast Cell Media for at least three weeks of incubation before checking surface expression of FcεRI and c-kit by flow cytometry.

Section 3: B Cell Culture and Analysis

-Glutamate-Free RPMI Media

The powder base was special ordered as a modification of RPMI (cat# 31800022 Life Technologies- Carlsbad CA) with L-Glutamic Acid and L-Glutamine removed. Media was prepared with the addition of 10% heat-inactivated FBS, 2mM L-Glutamine (cat# SH30034 HyClone- Logan, UT), 1mM Sodium Pyruvate (cat# SH30239 HyClone- Logan, UT), 1mM HEPES (cat# SH30237 HyClone- Logan, UT), 100 units/mL Penicillin G, 100μg/mL Streptomycin, 0.25μg/mL Amphotericin (Cat# SV30079 HyClone- Logan, UT), 50μM 2-Mercaptoethanol. pH to 7.4

-In vitro *Culture*

B220+ B cells were isolated from splenocytes using CD45R magnetic bead selection (Miltenyi Macs- Auburn, CA). Cells were plated at descending densities, starting at 20,000 cells/well in a final volume of 200μL glutamate-free RPMI. The cultures were stimulated with 1ng/mL IL-4 (Peprotech- Rocky Hill, NJ) and 1.25μg/mL anti-mouse CD40 (cat# 102902 BioLegend- San Diego, CA). After nine days of incubation, supernatants were harvested and analyzed for IgE levels by ELISA.

-IgE ELISA

Wells were coated with 5μg/mL B1E3, rat monoclonal anti-mouse IgE, for one hour at 37 degrees Celsius. Samples and standards were left overnight at four degrees Celsius. A biotinylated R1E4, anti-mouse IgE antibody, was incubated for one hour at 37 degrees Celsius. Streptavidin-AP was incubated for 45 minutes at 37 degrees Celsius. Following substrate addition, plates were read at 405-650nm.

Section 4: Mast Cell Migration Assay

-Migration Media

RPMI 1640 media was supplemented with 100 units/mL Penicillin G and Streptomycin (Cat# SV30079 HyClone- Logan, UT), 2mM L-glutamine (cat# SH30034 HyClone- Logan, UT), 1mM HEPES (cat# SH30237 HyClone- Logan, UT), and 1% BSA.

-Migration Assay Procedure

A portion of the experimental BMMC's were sensitized overnight with 1μg/mL anti-DNP IgE in normal Mast Cell Media, while the rest were left untreated. The next day, cells were washed to remove excess IgE then resuspended at $2e^6$/mL in Migration Media. 900uL of treated or control media was placed in the bottom of each appropriate well before inserting the filters (8um (cat# 3422) Polycarbonate Membrane Transwell Inserts by Corning) that were previously soaked for 60 minutes in Migration Media. 200μL of cells were carefully added on top of each filter then allowed to incubate for 4-6 hours. Treatment conditions included 1μg/mL SCF or negative control (migration media alone).

Cells were collected from the top of the filter and from the wells below in separate FACS tubes. Resuspended in the same volume (300μL PBS), the unstained cells were run on high

through BD FACSCanto™ II Analyzer for 60 seconds. Live cells were gated on, then the number of events from each run was used in the calculation below.

To calculate percent migration:

$$\frac{(Experimental\ well\ _{bottom}) - (Control\ well\ _{bottom})}{(Experimental\ well\ _{top}) + (Experimental\ well\ _{bottom})}\ x\ 100$$

where Experimental wells were those treated with SCF and Control wells with media alone.

Section 5: Mast Cell Enumeration

-Mast Cell Enumeration in Histology

Ear and backskin from three naive WT and KO mice were paraffin-embedded, mounted, and stained with Pinacyanol Erythrocyanate (PE) by Histo-Scientific Research Laboratories (Mt. Jackson, VA). 20 individual fields from each tissue sample were counted then averaged for each mouse. Data graphed based on the separate averages from three tissue replicates.

-Peritoneal Lavage Mast Cell Enumeration

After being sacrificed, mice were injected I.P. with 3mL of 0.1% BSA in cold PBS. The cavity was agitated for 30 seconds then the liquid was carefully recovered. Resulting cells were incubated for 5 minutes with Fc blocking reagent 2.4G2 (10μg anti-mouse unlabeled CD16/32) then stained for 20 minutes with anti-mouse APC-conjugated c-kit (clone 2B8) and anti-mouse FITC-conjugated FcεRI (clone MAR-1) (Biolegend- San Diego, CA). Cells were examined on a BD LSRFortessa, data analysis using FCS Express.

Section 6: Beta-Hexosaminidase Release Assay

-Beta-Hex Assay Buffer

Tyrode's Salt Solution (cat# T2397 Sigma- St. Louis, MO) was supplemented with 0.04% BSA and 5.6mM glucose.

-Beta-Hex Release Assay Procedure (adapted from published protocol[40])

Five million BMMC's, suspended at 500,000 cells/mL in normal mast cell media, were sensitized overnight with 1ug/mL anti-DNP IgE. The following day, cells were washed twice with PBS to remove excess antibody then resuspended at $10e^6$/mL in Assay Buffer.

100µL of cells (100,000/well) was added to each well in replicates then treated with 100µL of varying concentrations of DNP-BSA (0, 1, 5, 10, 50, 500). After a 30-minute incubation, the plate was spun to pellet the cells and stop the reaction. 100µL of supernatent was transferred to a new plate (this will be Percent). After discarding the remaining liquid, 100µL of 5% Triton X-100 was used to lyse the cells then transferred to the new plate (this will be Total).

All new wells were incubated with 50µL of 1mg/mL p-Nitrophenyl N-acetyl-β-D-glucosaminide (PNAG cat#N9376 Sigma- St. Louis, MO) in citrate buffer (40mM citric acid, 20mM sodium phosphate dibasic heptahydrate, pH to 4.5). After two hours, the reaction was stopped with 100µL of glycine buffer (400mM glycine, pH to 10.7). The plates were read at 405nm.

For each sample and its replicates, there will be two wells: Percent (supernatents alone) and Total (lysate after adding Triton X). The absorbances from both wells are used in the calculations below. The calculations must be repeated for each sample.

To calculate Total Mediator Content:

$$(Percent \times 2) + Total$$

To calculate percent mediator release:

$$\frac{(Percent \times 2)}{Total\ Mediator\ Content} \times 100$$

Section 7: Endothelial Cells

-Aortic Adventitia Digestion Enzyme Solution (AADES)

781.25 units of Collagenase Type II (cat# 17101-015 Life Technologies- Grand Island, NY) and 14.06 units of Elastase (cat# E7885 Sigma- St. Louis, MO) per 2.5mL PBS

-Aorta Dissociation Enzyme Solution (ADES)

125 units/mL Collagenase Type XI (cat# C7657 Sigma- St. Louis, MO), 60 units/mL Hyaluronidase Type 1-s (cat# H3506 Sigma- St. Louis, MO), 60 units/mL DNase I , 450 units/mL Collagenase Type I (cat# C0130 Sigma- St. Louis, MO)

-Isolating Aortic Endothelial Cells

The protocol used for enzymatic digestion of the aorta was published by Butcher et al[41]. Briefly, aortas underwent double-digestion to first break down the aortic adventitia (using AADES) then the aorta itself (using ADES). To get enough cells, aortas from four mice were pooled before being stained with anti-mouse APC-conjugated CD31 (clone 390) (Biolegend- San Diego, CA) and Histamine Receptors.

Section 8: Passive Systemic Anaphylaxis

-IgE-Mediated PSA

Female mice were sensitized with I.P. injections of 50μg anti-DNP IgE in 200μL saline. The next day, mice were challenged I.P. with 80ng DNP-BSA (cat# A23018 Life Technologies- Grand Island, NY) in 200μL saline. Using a murine rectal thermometer, an initial baseline temperature was taken, followed by time points of 10, 15, or 30 minutes apart as the experiment progressed. Mice were sacrificed two hours later by cardiac puncture.

-Histamine-Mediated PSA

Female mice were challenged I.P. with 50μg Histamine Dichloride (cat# H7250 Sigma, St. Louis, MO) in 200μL saline. Using a murine rectal thermometer, an initial baseline temperature was taken, followed by time points of 10, 15, or 30 minutes apart as the experiment progressed. Mice were sacrificed two hours later by cardiac puncture.

Section 9:* Nb *Infection

Graciously provided by Joe Urban (Agricultural Research Station—Beltsville, MD). Each experimental mouse was infected sub-cutaneously with approximately 650 stage 3 larvae. Fecal egg eggs were determined on days 6-9. Serum was collected by tail vein nick on days 7, 14, and 21.

Section 10: Freund's Adjuvant

-Complete Freund's Adjuvant

The CFA emulsion was prepared as 1 mg/mL heat-killed M. tuberculosis in mineral oil combined with 1 mg/mL Ovalbumin in PBS. Each mouse was injected sub-cutaneously with 100uL.

-Incomplete Freund's Adjuvant

Mice were injected I.P. with a 100μL mineral oil/Ovalbumin boost.

Section 11: Flow Cytometry and Statistical Analysis

-Flow Cytometry

Single-cell suspensions were incubated with Fc blocking reagent 2.4G2 (10μg unlabeled anti-mouse CD16/32) then stained on ice for 20 minutes with the appropriate anti-mouse fluoro-conjugated antibody. Washed and resuspended in PBS, cells were examined on an LSRFortessa or Canto (BD Bioscience). Data analysis was performed using FCS Express.

-Statistics

All statistical analysis was performed through GraphPad Prism. Two-group comparisons were calculated using unpaired two-tailed Student t-Tests, where p-values less than 0.05 were considered statistically significant. Data error bars represent the mean ± the standard deviation (SD) between samples.

-Chapter 3: Results-

KAR KO mice have higher IgE in vivo *and* in vitro

As reported by Ford et. al[42], 129/SvJ mice exhibit hyper-IgE due to mutations in its suspected negative regulator, CD23. To confirm the same phenomenon exists in the C57BL/6.129 mixed background, baseline IgE was determined by ELISA. Indeed when compared their C57BL/6 counterparts, the mixed background mice have higher levels of baseline IgE (Figure 3-1a). Another result to note is the increased level of baseline of IgE found in the KAR KO vs. WT, as this will become important later on.

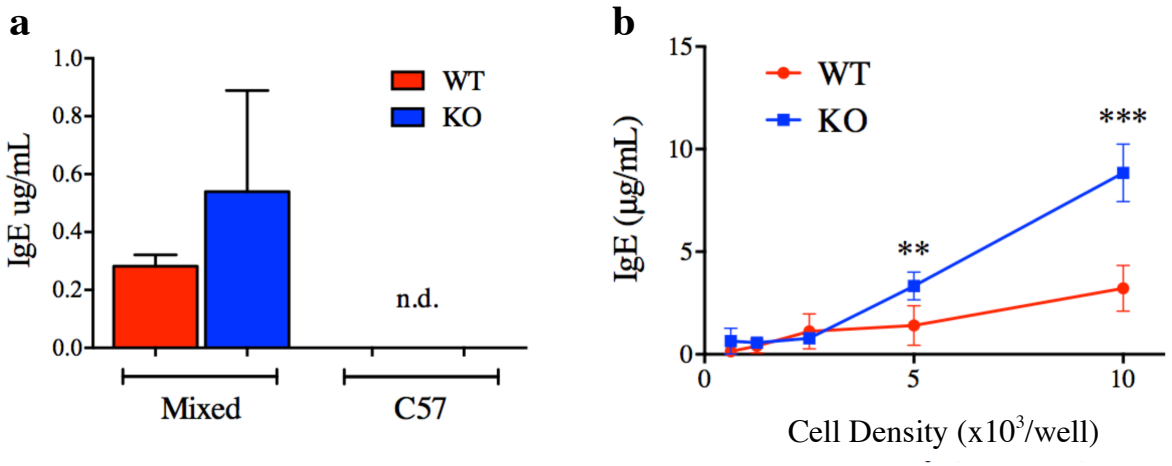

Figure 3-1. KAR KO mice produce more IgE. B6/129, or "mixed," background mice have higher *in vivo* baseline levels of serum IgE, while C57BL/6 background did not have detectable levels (a). Supernatents from *in vitro* stimulation of B6/129 splenic B cells showed more IgE production by KAR KO B cells (b).

Next, we sought to investigate if stimulated KAR KO B cells produce more IgE *in vitro*. Splenic B220+ cells were cultured in IL-4 and anti-CD40 for 9 days, then IgE levels measured by ELISA. Figure 3-1b shows a representative graph in which KO cells produced significantly more IgE upon stimulation *in vitro*. Together, these data show that B6/129 KAR KO mice have higher IgE levels *in vivo* as well as increased IgE produced *in vitro*.

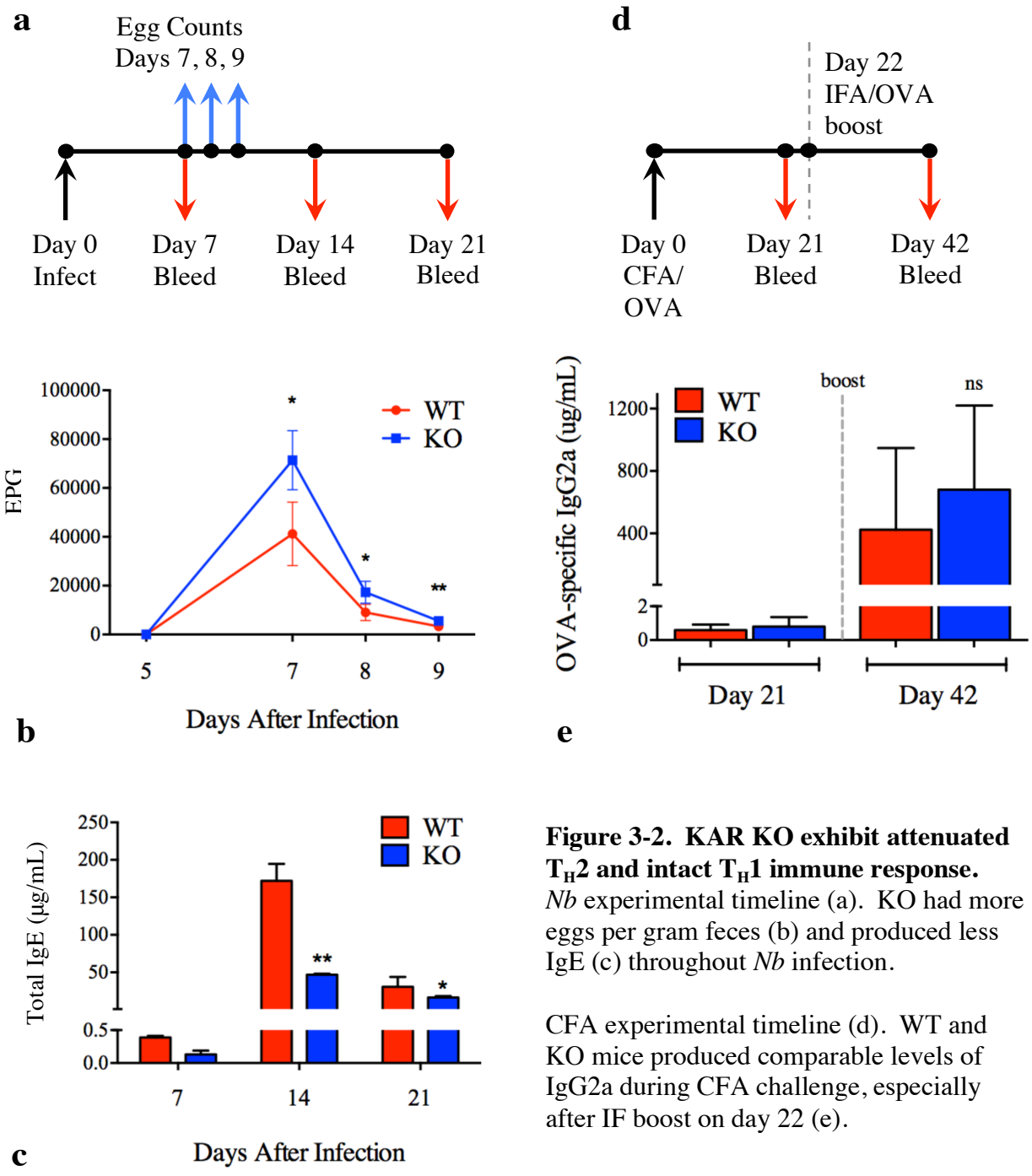

Figure 3-2. KAR KO exhibit attenuated T_H2 and intact T_H1 immune response. *Nb* experimental timeline (a). KO had more eggs per gram feces (b) and produced less IgE (c) throughout *Nb* infection.

CFA experimental timeline (d). WT and KO mice produced comparable levels of IgG2a during CFA challenge, especially after IF boost on day 22 (e).

KAR KO mice exhibit an attenuated T_H2 response

To determine if any T_H1/T_H2 skewing exists in KAR KO mice, two *in vivo* models were employed to test these two opposing immune responses. Once established, *Nippostrongylus brasiliensis* (*Nb*) prompts a robust T_H2 response from the host in order to

clear the infection. As shown in Figure 3-2b, KAR KO mice had significantly higher fecal egg counts at the peak of infection at day 7 and until the worms were cleared. Large numbers of eggs released in feces indicates the host did not effectively control and clear the parasite. KAR KO mice were also producing less IgE during the infection than the WT (Figure 3-2c). Althought IgE is not vital for clearing *Nb* infection, it is an important player in a T_H2 response. Together, these results suggest a deficit in the T_H2 leg of the KAR KO immune system.

Although CFA is not a live infection, as the active agent in the emulsion is heat-killed *M. tuberculosis*, the model induces a robust T_H1 response that can be further amplified by an IFA boost. Figure 3-2e shows no difference in antigen-specific IgG2a between WT and KAR KO, indicating they mounted comparable T_H1 immune responses.

Allergic Asthma and looking toward mast cells

As discussed in the Introduction, the T_H2 branch evolved as a defense mechanism against multicellular parasite, but is often inappropriately activated by environmental allergens. The *Nb* results prompted further investigation into the KAR KO immuno-phenotype; if the mice mounted a weaker response to *Nb*, then they should also develop a weaker sensitivity to allergens.

Mice were sensitized for two weeks, with five days intra-nasal (I.N.) administrations followed by two days rest then five more days of I.N. After two more days of rest, the animals were challenged with methacholine, a smooth muscle agonist, to measure Newtonian Resistance (R_n). This measurement indicates any resistance in the conducting airways, termed Airway Hyperreactivity (AHR).

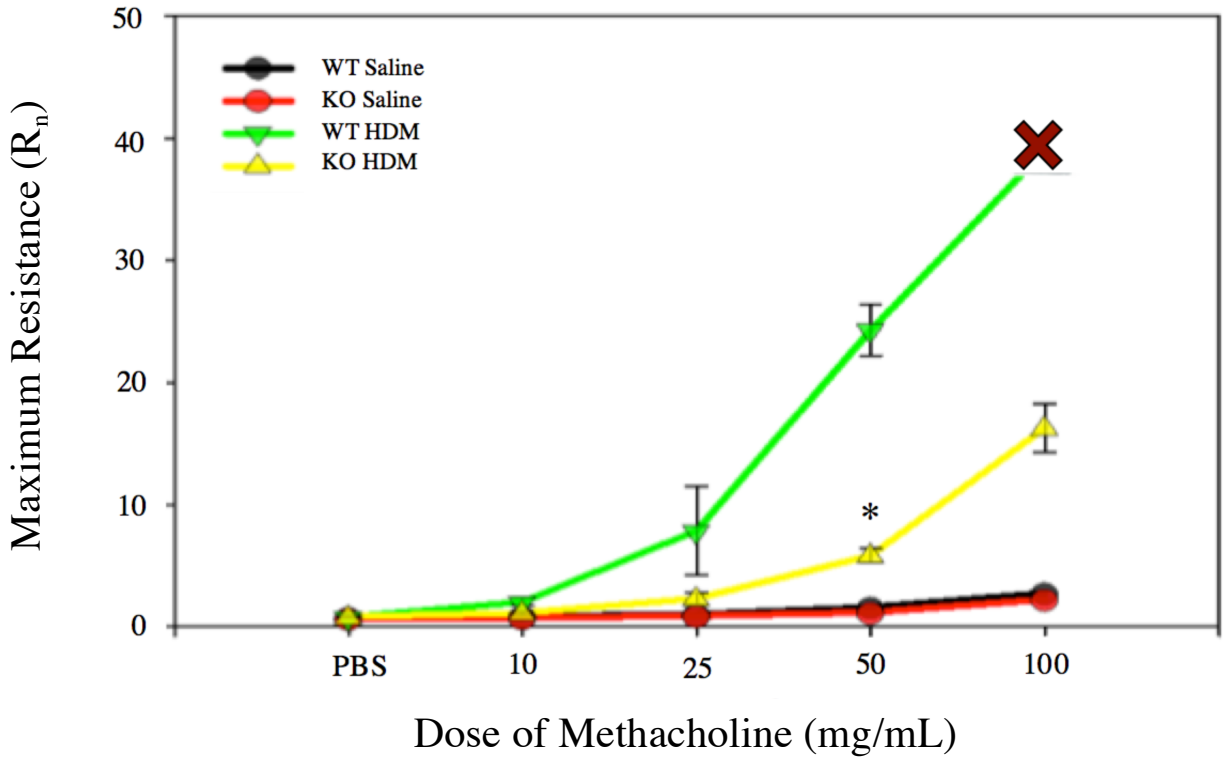

Figure 3-3. KAR KO mice develop a milder case of allergic asthma.
HDM-sensitized mice were challenged with increasing doses of the agonist Methacholine. AHR was determined by the maximium resistance measured within the lungs. Red X indicates animal death during challenge with indicated dose.
Units of Newtonian Resistance (R_n): $cmH_2O.s/mL$

WT mice succumbed to the highest dose of methacholine, as indicated by the red X, while the KO trailed with significantly lower AHR at each challenge. This experiment confirmed our hypothesis that KAR KO mice developed a milder case of allergic asthma. In addition, because AHR is mast cell-dependent, these results directed our attention toward the mast cell's role in the KAR KO phenotype.

Characterizing KAR KO mast cells

To determine if there was a difference in the number of tissue-resident mast cells, samples of ear and backskin were sectioned and stained with Pinacyanol Erythrocyanate (PE).

As seen in Figure 3-4, there was no difference in distribution (Figure 3-4a, b) or number (Figure 3-4c) of mast cells within the tissue. Peritoneal lavage, another source for enumeration, also showed comparable levels of mast cells (Figure 3-3d).

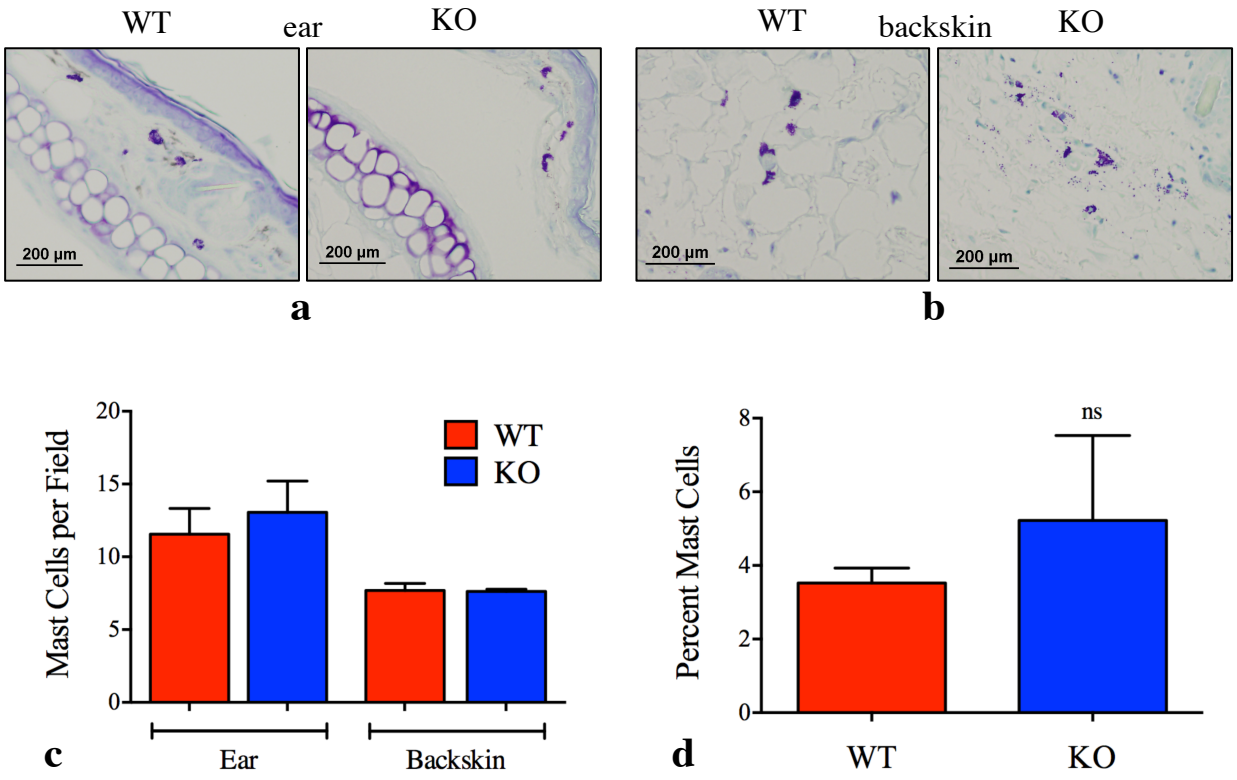

Figure 3-4. KAR KO mice have normal numbers of tissue-resident mast cells. Representative fields (20X) of mast cell distribution in ear (a) and backskin (b) tissues. Quantification of tissue-resident mast cells (c). Quantification of mast cells retrieved from peritoneal lavage (d).

Because it is difficult to obtain large numbers of mast cells from tissue, bone marrow-derived mast cells were used for further investigation. To verify the successful differentiation of both WT and KO BMMCs, analysis by flow cytometry showed equal surface expression of FcεRI and c-kit (Figure 3-5a, b). Correspondingly, there was no difference in ability to bind IgE (Figure 3-5c). In order to fully mature *in vivo*, committed progenitors must leave

circulation and enter the tissue. Upon exposure to the known mast cell chemotractant SCF, WT and KAR KO BMMC's migrated to the same extent *in vitro* (Figure 3-5d). These data suggest KAR KO hematopoietic cells differentiate appropriately into committed c-kit$^+$/FcεRI$^+$ mast cells.

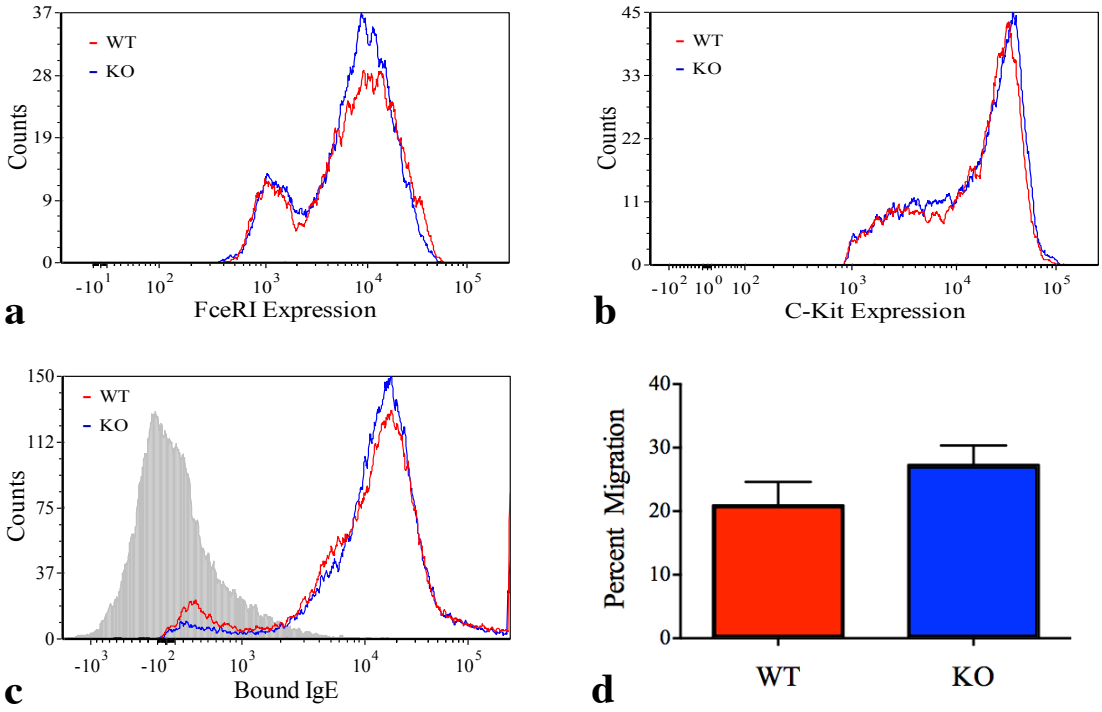

Figure 3-5 KAR KO BMMC's develop properly *in vitro*.
Surface expression of c-kit (a) and FcεRI (b) were comparable in WT and KO, indicating proper maturation of BMMC's. Both populations bound to IgE equally (c). WT and KAR KO BMMC's migrate properly toward SCF (d).

Next was to determine if KAR KO BMMC's degranulate properly to stimulus. Lysosomal-Associated Membrane Protein-1 (CD107a) is a heavily glycosylated protein found on the membrane of internal vesicles such as mast cell or cytotoxic granules as well as lysosomes. Upon membrane fusion and exocytosis, LAMP-1 can be detected on the cell surface and thus serves as a marker for degranulation. No difference in ability to degranulate was found during IgE- nor ionomycin-mediated release (Figure 3-6a).

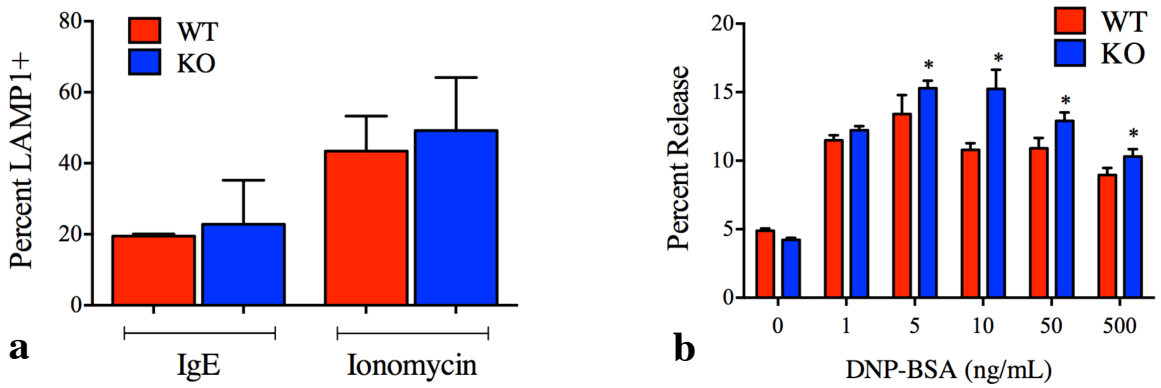

Figure 3-6 KAR KO BMMC's degranulate appropriately, but release more mediators. IgE-sensitized KAR KO BMMC's degranulated to the same extent as WT based on LAMP-1 surface expression (a). The percent release of beta-hexosaminidase, however, was increased in KO (b).

KAR KO mice exhibit severe anaphylaxis

IgE-mediated PSA is used to evaluate the mast cell's role in the systemic reaction. Age-matched female mice were sensitized overnight with anti-DNP IgE then anaphylaxis was triggered by DNP challenge. Although Figure 3-7a shows an apparent protection of KAR KO against a severe reaction, this interpretation was deemed invalid. As mentioned in Figure 3-1a, KAR KO mice have inherently high levels of circulating IgE. We hypothesize that the mast cells were already coated with non-specific IgE at the time of sensitization. As a result, less DNP-specific antibody was able to bind the mast cells and prompt degranulation upon antigen challenge.

In an attempt to circumvent this, an experimental group of mice were treated specially for three weeks, receiving frequent cage changes in an attempt to reduce exogenous antigens. We believed the conditions within the animal facility prompted an excess of antibody production in these mice, especially the knockouts. By the end of this period, the experimental mice had much lower levels of circulating IgE. KAR KO's had a three-fold

reduction to an average of 1.2 ug/mL IgE, while WT levels dropped below 0.03ug/mL. These experimental mice were then challenged with an IgE-mediated PSA. We chose to cardiac puncture within five minutes of administering the antigen in order to measure maximum histamine release within the serum. Figure 3-7c shows that KAR KO mice released significantly more histamine *in vivo* upon anaphylaxis.

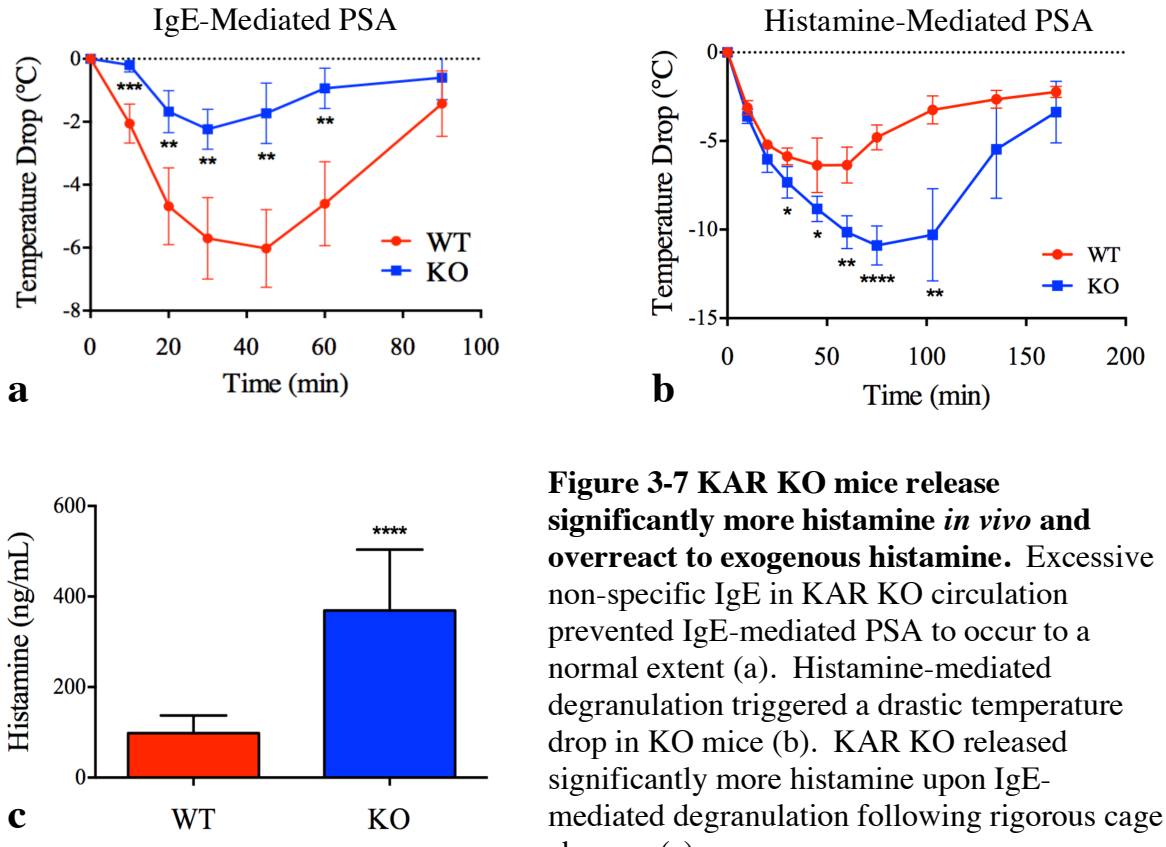

Figure 3-7 KAR KO mice release significantly more histamine *in vivo* and overreact to exogenous histamine. Excessive non-specific IgE in KAR KO circulation prevented IgE-mediated PSA to occur to a normal extent (a). Histamine-mediated degranulation triggered a drastic temperature drop in KO mice (b). KAR KO released significantly more histamine upon IgE-mediated degranulation following rigorous cage changes (c).

Histamine-mediated PSA is a way to bypass the mast cell and look at how other components within the system react. KAR KO mice experienced a drastic temperature drop and took longer to recover than WT (Figure 3-7b). This indicates that other physiological components are having exacerbated responses to endogenous or exogenous histamine.

Not only do KAR KO mice release excessive histamine *in vivo* upon IgE-mediated degranulation, tissues that respond to histamine also appear to overreact. Many cells

express histamine receptors (HR), most notably being the endothelial cells. Flow cytometry analysis showed no difference in HR expression on isolated aortic endothelial cells (Figure 3-8c) and although there was a slight shift on B cells (Figure 3-8a), splenic B and T cells (Figure 3-8b) had comparable levels of HR expression.

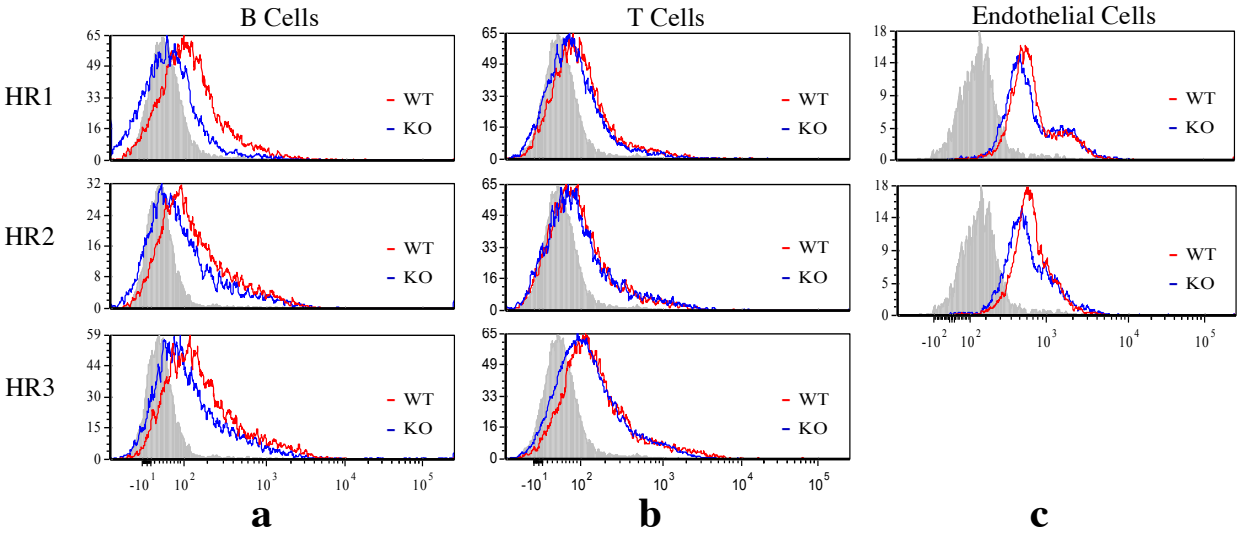

Figure 3-8. Histamine receptors are similarly expressed on B, T, and endothelial cells. Surface expression of histamine receptors 1, 2, and 3 on B cells (a), T cells (b), and aortic endothelial cells (c).

-Chapter 4: Discussion-

Mast cells are important immune cells that are involved in many protective inflammatory responses; unfortunately they can also contribute to immune diseases. Anaphylaxis is a direct result of systemic mast cell activation, the severity of which stems from vasoactive histamine. This and other inflammatory mediators released upon mast cell degranulation also cause the well-recognized symptoms of allergies—runny nose and sneezing, and asthma—wheezing and difficulty breathing.

With normal circulating glutamate levels reaching 30-100uM[33], many research groups have begun to study the existence of glutamate receptors outside of the central nervous system (CNS). This report finds that disrupting the formation of functional kainate receptors (KAR) has unexpected consequences on immune components, specifically mast cells.

Figure 3-1a showed that mice of the B6/129 mixed background have an elevated IgE baseline compared to their C57BL/6 counterparts. As discussed in the Introduction, the negative IgE regulator CD23 is mutated 129/SvJ mice, resulting in excessive IgE in circulation. For KAR KO's, this excessive antibody production is further amplified above the WT baseline. This was also seen *in vitro* when stimulated KAR KO splenic B cells consistently produced more IgE. It is unclear if this amplification is seen in other isotypes apart from IgE, though a simple *in vitro* experiment could determine this. In addition, future work on this project will transition toward using KAR KO mice on the C57BL/6 background to resolve the issue of excessive IgE circulating in 129 strains

Previous work done in our lab showed that glutamate (Glu) and kainic acid (KA) treatments *in vitro* increased IgE production by human B cells, a phenomenon that could be

abrogated by the KAR-specific antagonist, NS102. Data not presented in this report showed inconsistent responses by purified murine KAR KO B cells to Glu and KA treatments *in vitro*. The experiments consistently showed that WT B cells responded to treatments with increased IgE production. During some of these experiments, the KAR KO B cells acted as predicted: there was no increase in IgE because they lack the KAR receptor. Many experimental repeats, however, showed similar increases in IgE production by both the WT and KO B cells. After much troubleshooting, there still isn't a firm conclusion about the effects of kainic acid on murine B cells.

We sought to characterize the KAR KO immune responses, specifically the T_H2/T_H1 paradigm. When challenged with the parasite *Nippostrongylus brasiliensis* (*Nb*), KAR KO mice produced less IgE while mounting the appropriate response (Figure 3-2c). Although IgE is not necessary for *Nb* clearance, this result suggests a deficit in the KAR KO T_H2 immune response. Furthermore, because the mice were unable to mount a complete T_H2 response, the worms were not cleared as effectively as WT. As a result, KAR KO had higher egg counts for the duration of the infection (Figure 3-2b).

Indeed the results from the allergic asthma model further support this hypothesis. House Dust Mite (HDM)-sensitized WT mice developed such severe disease, they died upon high doses of methacholine challenge. KAR KO mice not only survived agonist challenge, they had airway resistance significantly below WT (Figure 3-3). It is important to note that KAR KO mice still developed allergic disease, as is evidenced by their saline counterparts. As discussed in the Introduction, allergies result from an inappropriate T_H2 response. This thesis argues that KAR KO mice have an attenuated T_H2 immune response, as seen by 1) reduced ability to clear *Nb* infection and 2) the development of an alleviated HDM sensitivity.

Next we looked toward the other end of the paradigm, the T_H1 branch. WT and KAR KO were injected with heat-killed *M. tuberculosis* to trigger Toll-Like Receptor (TLR) activation. The mice mounted equivalent responses to the challenge and boost of Freund's Adjuvant. In this case, OVA-specific IgG2a showed no difference between WT and KAR KO T_H1 responses (Figure 3-2e). Combined with the findings discussed above, we concluded that KAR KO mice have an attenuated T_H2 response with an intact T_H1 response. This hypothesis had exciting potential with clear clinical relevance; current allergy treatments are generally immune-suppressive and leave the patient vulnerable to other infections. The phenotype seen in KAR KO mice suggested a novel protein target that could weaken an overzealous T_H2 branch to block allergies, while preserving the T_H1 branch that's protective against infections such as influenza and tuberculosis. Reflecting back on these experiments, we were drawn toward the role that mast cells may be playing.

Beginning *in vivo*, we found that mast cells in the skin stained appropriately and had normal distribution and general morphology (Figure3-4). These samples were taken during naïve conditions, however, and do not speak to the mast cells' ability to expand during infection. Gut sections from *Nb*-infected mice or lung sections from HDM-sensitized mice would give further insight into how the mast cells function upon challenge.

Because it's difficult to obtain large amounts of mature mast cells from the animal, bone marrow-derived mast cells were used for further investigation. Firstly, WT and KAR KO bone marrow progenitors matured into proper mast cells as indicated by comparable surface expression of FcεRI and c-kit (Figure 3-5a, b). Subsequent experiments showed several equalities between WT and KO BMMC's: 1. ability to bind IgE (Figure 3-5c), 2. migration toward a chemotractant (Figure 3-4d), and 3. percent degranulation as determined by surface

LAMP-1 expression (Figure 3-6a). It was concluded that KAR KO mast cells mature, migrate, and activate appropriately *in vivo* and *in vitro*.

Differences arise, however, when quantifying the amount of mediators released from mast cell granules. Significantly more beta-hex was measured from KAR KO BMMC's compared to WT (Figure 3-6b). IgE-mediated PSA also resulted in drastic amounts of histamine released into circulation of KAR KO mice (Figure 3-7c). These data merit further investigation into the contents of mast cell granules. Early mediators, such as histamine and TNF-α, and late mediators, such as IL-13, should be measured from IgE-activated BMMC's as well as serum collected early and late during PSA experiments. This information would help to characterize both the immediate and delayed phases of anaphylaxis.

While both the *Nb* and CFA models gave basic insight into how KAR KO mice respond to T_H2 vs. T_H1 challenges, there are many more components to these immune responses that were not examined. Indeed, neither IgE nor mast cells are absolutely necessary for the clearance of *Nb* infections, yet there was a clear deficiency in the KAR KO's response as indicated by the higher fecal egg counts. These experiments must be repeated to look at cytokine expression and involvement of other immune cells in order to make firm conclusions about these immune branches.

The results from the allergic asthma model are also intriguing and there is much more data to collect from this type of experiment. Shannon Li et. al[43] published a three-week HDM-sensitization protocol that induces much more mast cell expansion within the lungs. This model better mimics the pathology seen in human allergic asthma. As discussed in the Introduction, chronic disease marked by prolonged inflammation causes irreversible lung and airway damage. Methacholine challenge is used to evaluate bronchoconstriction due to this airway remodeling,

and thus is an assessment of the late phase reaction. Challenging with HDM extract, on the other hand, can be used to assess the early phase reaction by measuring tissue dampening (G) and lung elastance (H), which are indicative of acute phase bronchospasms. This line of experiments would allow a thorough examination of the disease state and how KAR KO differ from WT.

Because the issue of elevated non-specific IgE was not realized until late, all IgE-mediated anaphylaxis must be repeated in order to collect true temperature drops based on full mast cell degranulation. The experimental mice that received frequent cage changes showed surprising amounts of histamine released upon IgE-mediated PSA, but because cardiac puncture was performed within five minutes, no temperature readings were acquired from these mice.

It is surprising that in addition to excessive histamine being released *in vivo*, KAR KO mice also show an exaggerate response to exogenous histamine treatments. The detection of histamine receptors on endothelial cells needs to be repeated, as it was only performed once due to the necessity of pooling four mice. We expected to find higher expression of histamine receptors (HR) in KAR KO mice to explain the exaggerated response, but there was no difference found on aortic endothelial cells. A Mile's Assay will be performed to quantify vascular leakage resulting from histamine-mediated passive cutaneous anaphylaxis (PCA).

In summary, this report presents preliminary findings from the immuno-characterization of KAR KO mice. Many experiments discussed will be expanded in the future to acquire more in-depth data; this includes cytokine production *in vivo* and *in vitro*, histology from *Nb* and asthma models, additional mediator release assays, as well as the continued investigation into histamine receptors. Although there initially appeared to be clinical potential for a kainate receptor antagonist to attenuate allergies, the adverse response to histamine may limit this

prospect. Overall, the unique KAR KO phenotype is interesting and could provide new insight into the balance between different branches of the immune system.

-References-

1. Murphy K. *Janeway's Immunobiology*. 8th ed. New York; 2012.

2. Adkinson FJ. *Middleton's Allergy: Principles and Practice*. 8th ed. Philadelphia: Elsevier Saunders; 2014.

3. Gurish M, Castells M. Mast Cell Derived Mediators. 2013. http://www.uptodate.com/contents/mast-cell-derived-mediators.

4. Janeway CJ, Travers P, Walport M. *Immunobiology: The Immune System in Health and Disease*. 5th ed. New York: Garland Science; 2001.

5. Lieberman P. Biphasic anaphylactic reactions. *Ann Allergy, Asthma, Immunol*. 2005;95:217-226.

6. Anthony R, Rutitzky L. Protective Immune Mechanisms in Helminth Infection. *Nat Rev Immunol*. 2007;7(12):975-987.

7. Rowe B, Gaeta T, Tintinalli J. Anaphylaxis, Acute Allergic Reactions, and Angioedema. In: *Tintinalli's Emergency Medicine: A Comprehensive Study Guide*. 7th ed. New York: McGraw-Hill; 2011.

8. Mosmann T, Coffman R. Two Types of Mouse Helper T Cell Clone. *Immunol Today*. 1987;8(7):223-227.

9. Kidd P. Th1/Th2 Balance: The Hypothesis, its Limitations, and Implications for Health and Disease. *Altern Med Rev*. 2003;8(3):223-246.

10. Gwilz. Vector diagram of laboratory mouse. *Wiki Media Commons*. 2013.

11. Remesz O. Human esophagus, connecting pharynx to stomach. *Wiki Media Commons*. 2007.

12. Saburchill. Roundworm Phylum: Trichinella. *Open Door Web Site*.

13. Camberis M, G LG, Urban J. Animal Model of Nippostrongylus brasiliensis and Heligomosomoides polygyrus. In: *Current Protocols in Immunology*. John Wiley & Sons, Inc.; 2003.

14. Rabinowitsch L. Zur Frage des Vorkommens von Tuberkelbacillen in der Marktbutter. *Zeitschrift fuer Hyg*. 1897;26:90-111.

15. Freund J, Bonanto M. The Effect of Paraffin Oil, Lanolin-Like Substances and Killed Tubercle Bacilli on Immunization with Diptheric Toxoid and Bact. Typhosum. *J Immunol*. 1944;48:325-334.

16. Friedewald WF. Enhancement of the Immunizing Capacity of Influenza Virus Vaccines With Adjuvants. *Science*. 1944;99(2579):453-454. doi:10.1126/science.99.2579.453.

17. Friedewald W. Adjuvants in Immunization with Influenza Virus Vaccines. *Proc Soc Exp Biol Med*. 1944;80:477-491.

18. Henle W, Henle G. Effect of Adjuvants on Vaccination of Human Beings Against Influenza. *Proc Soc Exp Biol Med*. 1945;59(179-181).

19. Billiau A, Matthy P. Modes of Action of Freund's Adjuvants in Experimental Models of Autoimmune Diseases. *J Leukoc Biol*. 2001;7:849-860.

20. Castro A. Adjuvant treatment increases the resistance to Mycobacterium avium infection of mycobacteria-susceptible BALB/c mice. *Clin Exp Immunol*. 1993;92(3):466-472.

21. Guy B. The Perfect Mix: Recent Progress in Adjuvant Research. *Nat Rev Microbiol*. 2007;5:505-517.

22. Nimmerjahn F, Ravetch J. Fc-Receptors as Regulators of Immunity. *Adv Immunol*. 2007;96:179-204.

23. Szalai A, Hu X, Raman C, Barnum S. Requirement of the Fc receptor common gamma-chain for gamma-delta T cell-mediated promotion of murine experimental autoimmune encephalomyelitis. *Eur J Immunol*. 2005;35:3487-3492.

24. Blank U, Rivera J. The ins and outs of IgE-dependent mast-cell exocytosis. *Trends Immunol*. 2004;25(5):266-273. doi:10.1016/j.it.2004.03.005.

25. Gilfillan A, Austin S, Metcalfe D. Mast Cell Biology: Introduction and Overview. *Adv Exp Med Biol*. 2011;716:2-12.

26. Rous P. A sarcoma of the fowl transmissible by an agent separable from the tumor cells. *J Exp Med*. 1911;13:397-411.

27. Parsons S, Parsons T. Src Family Kinases, Key Regulators of Signal Transduction. *Nat Publ Gr*. 2004;23:7906-7909.

28. Gilfillan A, Tkaczyk C. Integrated Signalling Pathways for Mast-Cell Activation. *Nat Rev Immunol*. 2006;6:218-230.

29. Parravicini V, Gadina M, Kovarova M. Fyn kinase initiates complementary signalis required for IgE-dependent mast cell degranulation. *Nat Immunol*. 2002;3(8):741-748.

30. Putney Jr J. Capacitative Calcium Entry: Sensing The Calcium Stores. *J Cell Biol*. 2005;169(3):381-382.

31. Putney JJ. Capacitative Calcium Entry: From Concept To Molecules. *Immunol Rev*. 2009;321:10-22.

32. Antibody Structure and Classes of Immunoglobulins. *Thermo Fish Sci Inc*. 2015.

33. Gill S, Pulido O. *Glutamate Receptors in Peripheral Tissue: Excitatory Transmission Outside the CNS*. New York: Kluwer Academic / PlenumPublishers; 2005.

34. Said S, Berisha H, Pakbaz H. Excitotoxicity in the lung: N-Methyl-D-aspartate-induced, nitric oxide-dependent, pulmonary edema is attenuated by vasoactive intestinal peptide and by inhibitors of poly(ADP-ribose)polymerase. *Proc Natl Acad Sci USA*. 1996;93(10):4688-4692.

35. Said S. Glutamate receptors and asthmatic airway disease. *Trends Pharmacol Sci*. 1999;20(4):132-135.

36. Inagaki N, Kuromi H, Gonoi T. Expression and role of ionotropic glutamate receptors in pancreatic islet cells. *FASEB J*. 1995;9(8):686-691.

37. Miglio G, Varsaldi F, Lombardi G. Human T lymphocytes express N-methyl-D-aspartate receptors functionally active in controlling T cell activation. *Biochem Biophys Res Commun*. 2005;338(4):1875-1883.

38. Tsai L, Lee Y, Wu J. Role of N-methyl-D-aspartate receptors in gastric mucosal blood flow induced by histamine. *J Neurosci Res*. 2004;77(5):730-738.

39. Brand J. Transduction mechanisms for the taste of amino acids. *Physiol Behav*. 1991;49(5):899-904.

40. Sabban S, Ye H, Helm B. Development of an in vitro model system studying the interaction of Equus caballus IgE with its high affinity FceRI receptor. *J Vis Exp*. 2014;(93). e52222, doi:10.3791/52222

41. Butcher MN, Herre M. Flow cytometry analysis of immune cells within murine aortas. J Vis Exp. 2011;(53). pii: 2848. doi: 10.3791/2848.

42. Ford JW, Sturgill JL, Conrad DH. 129/SvJ mice have mutated CD23 and hyper IgE. *Cell Immunol*. 2009;254(2):124-143

43. Li S, Aliyeva M, Daphtary N. Antigen-indeuced mast cell expansion and bronchoconstriction in a mouse model of asthma. *Am J Physiol Lung Cell Mol Physiol*. 2014;306:L196-L206

-Vita-

Andrea Elkovich was born in Robbinsdale, MN in 1988. Raised in Chesterfield, VA, she graduated in 2007 from Lloyd C. Bird's Pre-Engineering high school specialty center. In May 2011, Andrea received dual Bachelor Degrees in Biomedical Engineering and Biology, with a minor in chemistry, from Virginia Commonwealth University. In August 2013, she entered VCU School of Medicine's Microbiology and Immunology Master's program. Here she joined Dr. Daniel Conrad's lab to study the immune system of Kainate Receptor knockout mice. Upon successful defense of her master's thesis, Andrea will enter the VCU Biomedical Sciences Doctoral Program where she will continue her research in the Conrad Lab.